Hindawi Publishing Corporation
Journal of Nanomaterials
Volume 2013, Article ID 232409, 9 pages
http://dx.doi.org/10.1155/2013/232409

Research Article

Optical Property Characterization of Novel Graphene-X (X=Ag, Au and Cu) Nanoparticle Hybrids

Sumit Ranjan Sahu,[1] Mayanglambam Manolata Devi,[1] Puspal Mukherjee,[2] Pratik Sen,[2] and Krishanu Biswas[1]

[1] *Department of Materials Science and Engineering, Indian Institute of Technology Kanpur, Kanpur 208016, India*
[2] *Department of Chemistry, Indian Institute of Technology Kanpur, Kanpur 208016, India*

Correspondence should be addressed to Krishanu Biswas; kbiswas@iitk.ac.in

Received 6 August 2013; Accepted 29 September 2013

Academic Editor: Pathik Kumbhakar

The present investigation reports new results on optical properties of graphene-metal nanocomposites. These composites were prepared by a solution-based chemical approach. Graphene has been prepared by thermal reduction of graphene oxide (GO) at 90°C by hydrazine hydrate in an ammoniacal medium. This ammoniacal solution acts as a solvent as well as a basic medium where agglomeration of graphene can be prevented. This graphene solution has further been used for functionalization with Ag, Au, and Cu nanoparticles (NPs). The samples were characterized by X-ray diffraction (XRD), Raman spectroscopy, UV-Vis spectroscopy, scanning electron microscopy (SEM), and transmission electron microscopy (TEM) to reveal the nature and type of interaction of metal nanoparticles with graphene. The results indicate distinct shift of graphene bands both in Raman and UV-Vis spectroscopies due to the presence of the metal nanoparticles. Raman spectroscopic analysis indicates blue shift of D and G bands in Raman spectra of graphene due to the presence of metal nanoparticles except for the G band of Cu-G, which undergoes red shift, reflecting the charge transfer interaction between graphene sheets and metal nanoparticles. UV-Vis spectroscopic analysis also indicates blue shift of graphene absorption peak in the hybrids. The plasmon peak position undergoes blue shift in Ag-G, whereas red shift is observed in Au-G and Cu-G.

1. Introduction

Graphene is a unique allotrope of carbon characterized by honeycomb lattice of sp^2-hybridized carbon atoms in which carbon atoms are packed in a two-dimensional (2D) hexagonal lattice [1]. Graphene, often considered as a "miracle material" of the 21st century, has attracted tremendous attention in the academic community [2]. Being one-atomic layer thick sheet of carbon extending infinitely in 2D, its properties encompass range of superlattices. This includes high value of Young's modulus (~1100 GPa) [3], fracture strength (125 GPa) [3], thermal conductivity (~5000 W/mK) [4], mobility of charge carriers (2×10^5 cm^2/Vs) [5], and specific surface area 2630 (m^2/g) [6]. Owing to its excellent physical and chemical properties, graphene is considered as a potential candidate for large number of applications in many technological fields such as nanoelectronics [7], composites [8], energy storage devices [6], efficient lasers, photodetectors, and biomedical applications [9].

Preparation of high quality graphene is needed to study the unique properties for applications. A number of different ways of preparing graphene have been reported in the literature [10]. This includes micromechanical exfoliation of graphite [11], chemical vapor deposition [12], and chemical methods to create colloidal suspension [13]. The micromechanical method is time consuming, and the yield is low and thus limits our ability to have significant economic and technological impact [11]. On the other hand, graphene is prepared via solution chemistry involving oxidation of graphite to prepare layered graphene oxide sheets (GOS), which can further be reduced to obtain graphene sheets (GS). GS can be considered as chemically modified sheets having controllable electronic properties. However, unless these sheets are well separated from each other, the graphene sheets tend to form

agglomerates or even restack to form graphite due to Van der Waals interaction [14, 15]. Thus, the addition of any dispersoid which can bind tightly onto graphene sheets is of utmost necessity to achieve better dispersion of graphene sheets. In this context, decoration of graphene with metal nanoparticle becomes very important. Very recently, integration of graphene and metal nanoparticle to prepare new generation of hybrid nanomaterials has aroused extensive interest for large number of potential applications like chemical sensors, energy storage and catalysis, as well as hydrogen storage [16–21]. Most notably, noble metal nanoparticles (NP) have widely been used as a catalyst to promote various chemical reactions [22]. Catalyst support is found to be an important aspect affecting the catalytic activity of the catalyst [23]. To enhance the catalytic activity, graphene-metal nanoparticle hybrid composite can be used due to its very high specific surface area.

In the light of recent studies carried out by different groups on decoration of NPs with graphene to prepare hybrid structure, we consider that it is important to investigate the influence of metal nanoparticles on the electronic structure of graphene. For this purpose, we have synthesized gold (Au-G), silver (Ag-G), and copper nanoparticle decorated-graphene (Cu-G) via chemical synthesis. Almost all the previous works had generally dealt with synthesis of such hybrid structure [24, 25]. The nature of interaction between graphene and NPs is not properly studied. In this work, we have employed both Raman and UV-Vis spectroscopic techniques to obtain optical properties of the nanomaterials, and thereby electronic structures of the materials are brought about.

2. Experimental Procedure

2.1. Materials. Graphite powder (100 mesh, 99.9995%), silver nitrate ($AgNO_3$, 99.9%), hydrogen tetrachloroaurate (III) hydrate ($HAuCl_4$, 99.9%), copper sulfate ($CuSO_4$, 99.9%) (Alfa Aesar, India), sodium nitrate ($NaNO_3$), potassium permanganate ($KMnO_4$), concentrated sulfuric acid (H_2SO_4), ammonia solution (NH_4OH), hydrazine hydrate solution ($H_2NNH_2{\cdot}H_2O$) and hydrogen peroxide (H_2O_2) (Sigma Aldrich, India), Trisodiumcitrate dehydrate ($C_6H_5Na_3O_7{\cdot}H_2O$), Dextrose ($C_6H_{12}O_6$), and Sodium hydroxide (NaOH) (Merck Millipore, India) were used for the preparation of graphene and nanocomposites. All the chemicals were used in the condition as received without further purification. The water used in all the experiments was purified through a Millipore system.

2.2. Preparation of Graphite Oxide. Graphite oxide was prepared by modified Hummers method [26] by taking 2 g of natural graphite powder in a 250 mL beaker placed in an ice bath, maintaining the temperature at 20°C. Subsequently, 1 g of $NaNO_3$, 46 mL of H_2SO_4, and 6 g of $KMnO_4$ were added slowly to the graphite powder and kept under stirring for 15 min. After that, the ice bath was removed, and the solution was heated at 35°C for 30 min. Then, 92 mL of distilled water was added slowly into the solution and stirred for further 30 min. Finally, 80 mL of hot distilled water was added, followed by the addition of 30% H_2O_2 aqueous solution until the bubbling disappeared and the colour of the solution turned to deep yellow. The residue was collected after centrifugation, and warm water was utilized for subsequent washing to make it neutral (pH = 7). The resulting powder was redispersed into distilled water by ultrasonication for 30 min. The solution was freeze dried to get the desired brown coloured graphite oxide powder.

2.3. Exfoliation and Reduction of Graphene Oxide (GO). The exfoliated GO was prepared by ultrasonicating 0.01 g of the synthesized graphite oxide powder in 100 mL of distilled water in a 250 mL round-bottom flask for 2 h. The pH of the so obtained yellow brown suspension of GO was adjusted to the value of 10 by dropwise addition of 315 μL of 25% ammonia solution into it. For reduction of GO, 35 μL of hydrazine hydrate was added slowly, and the whole suspension was refluxed in an oil bath at 90°C for 2 h while stirring. Finally, black coloured precipitate of graphene (G) obtained after centrifugation was redispersed in distilled water and kept as a stock solution for the synthesis of Ag-G, Au-G, and Cu-G.

2.4. Preparation of Ag-G, Au-G, and Cu-G. The synthesis of Ag-G has been carried out according to the method described by Mao et al. [27]. Equal volume (20 mL) of graphene stock solution and silver nitrate aqueous solution (0.001 M) were slowly mixed in a 250 mL round-bottom flask. The whole solution was heated to 90°C with subsequent addition of 2 mL sodium citrate (w/v 1%) aqueous solution into it while stirring for 15 min to complete the reaction. After cooling down to room temperature, the solution was centrifuged many times with ethanol and water until the undesired by-products are removed, and the precipitate was redispersed in distilled water. Au-G was also prepared in similar fashion by mixing equal volume (20 mL) of graphene solution and $HAuCl_4$ aqueous solution (0.001 M) followed by the addition of 2 mL of 38.8 mM sodium citrate aqueous solution. Cu-G was prepared by the following method. 2.4 g of dextrose was dissolved in 30 mL of water. 60 μL of 1.0 M NaOH solution and 1 mL of graphene stock solution were added to it. The whole mixture was heated to 80°C under stirring in argon atmosphere. 1.2 mL of copper sulfate aqueous solution (0.01 M) was added to it. After five minutes of constant stirring at 80°C, Cu-G was obtained.

3. Characterizations

X-ray diffraction (XRD) of all the powder samples were recorded by a Bruker D8 focus X-ray diffractometer with Cu K_α radiation (λ = 0.154056 nm) operating at 40 KV and 20 mA. To investigate structural change during chemical processing, the Raman spectra were recorded with a WITec GmbH alpha 300 R Raman spectrometer in the back-scattering mode using an Ar-ion laser (514.5 nm) as an excitation source. The UV-Visible absorption spectra of aqueous solutions of GO, G, Ag-G, Au-G, and Cu-G were recorded in the range between 200 and 800 nm using

a Jasco V-670 UV-Vis spectrophotometer. Scanning electron microscopic (SEM) and Transmission electron microscopic (TEM) micrographs of G, Ag-G, Au-G, and Cu-G were taken with a Carl Zeiss EVO 50 VP scanning electron microscope and FEI Tecnai G^2 U-twin 200 KV instrument, respectively, to observe the nanoscale microstructure.

4. Results and Discussions

In the following, we shall describe the results obtained during present investigation and discuss the results in the light of the available literature.

4.1. Structural Characterization

4.1.1. X-Ray Diffraction (XRD). X-ray diffraction patterns of graphene oxide (GO), graphene (G), and graphene silver (Ag-G) nanoparticles hybrid materials are presented in Figure 1. XRD pattern of GO shows a sharp diffraction peak at $2\theta = 14.03^\circ$ corresponding to (001) of GO. The XRD pattern of G shows two distinct peaks at $2\theta = 24^\circ$ and 44.8°, which are attributed to (002) and (100) reflections of graphene nanosheets. The calculated d-spacing of graphene using broad peak is 0.364 nm. The broadness of the peak signifies decrease in the crystallinity of graphene upon reduction from GO. On the other hand, XRD pattern of Ag-G reveals the peaks due to (111), (200), (220), and (311) of Ag nanocrystals as well as broad peak (002) due to graphene. Similar observation has been made for Au-G and Cu-G nanohybrids. No peaks corresponding to oxides of Ag, Au, or Cu are observed within the detectable limit of XRD. The peaks due to metal nanocrystals are broad, indicating nanocrystalline size and strain due to incorporation within graphene nanosheet. The position of (002) peak of graphene does not change for different metal hybrids. Using the peak position of graphene, the calculated d-spacing of Ag-G is 0.370 nm, whereas d_{002} of graphite is 0.335 nm. The broadness of the peak is the indication of the presence of graphene nanosheets with varying d-spacing values.

4.1.2. Scanning (SEM) and Transmission Electron (TEM) Microscopic Observation. The detailed microstructural characterization of graphene and graphene-metal nanoparticle hybrids has been carried out using SEM and TEM. Figure 2(a) shows high resolution SEM micrograph of graphene and reveals crumbled and scrolled morphology of graphene sheets. Thin sheet of graphene crumbled into different layers is clearly visible in the Figure 2(a). Figures 2(b), 2(c), and 2(d) are the SEM images of graphene-metal hybrids, that is, Ag-G, Au-G, and Cu-G. The figure shows that the metal nanoparticles appear as discrete bright dots, which are homogeneously distributed on the surface of the graphene sheets. The graphene and graphene-metal nanoparticle hybrids are characterized directly under SEM without coating by gold film, suggesting their conductive nature. The detailed morphology and structure of the graphene-metal nanoparticle hybrids have been characterized by TEM. It is to be noted that TEM samples were prepared by dropping the sonicated dispersion

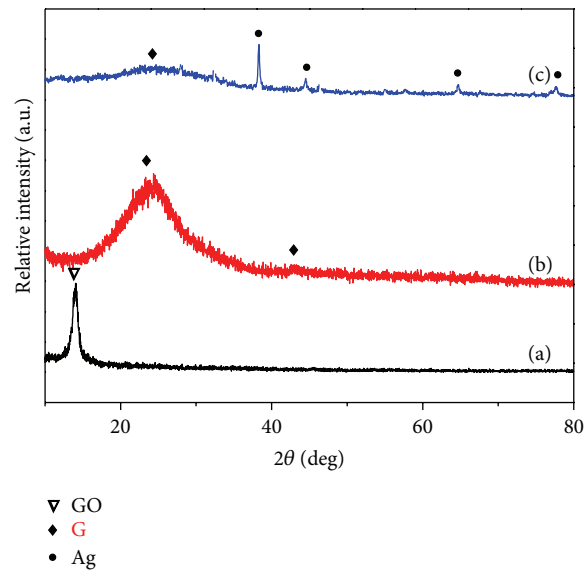

Figure 1: XRD patterns of (a) GO (b) G, and (c) Ag-G.

of sample in ultrapure methanol onto 600 mesh copper grids coated with lacy carbon and dried at room temperature for 3 hours. As observed in Figure 3(a), graphene nanosheets are randomly compact and stacked, revealing uniform laminar morphology such as crumbled silk veil waves. The selected area diffraction pattern (SADP) obtained from such nanosheets is shown as inset in Figure 3(a). The SADP reveals two diffraction rings, which can be indexed using (100) and (002) of graphene. Therefore, the formation of graphene by the reduction of graphene oxide is confirmed from the SADP pattern. Figures 3(b), 3(c), and 3(d) reveal graphene-metal nanoparticles hybrid composite with Ag, Au, and Cu used as nanoparticles to decorate the graphene nanosheets. Figure 3(b) shows scrolled morphology of graphene sheets with distributed Ag nanoparticles, embedded within the graphene sheets. The multiple stacking of graphene consisting of uniformly distributed Ag nanoparticles with average size of 25 ± 5 nm is distinctly observed. The histogram (as shown in the bottom inset) corroborates the narrow size distribution with maximum number of particles around 25 nm along with few larger particles of about 30 nm. The SADP obtained from the hybrid nanocomposite is shown as inset in Figure 3(b). The sharp diffraction rings can be indexed as those of Ag, while diffraction rings corresponding to (100) and (002) of graphene can also be deciphered. Figure 3(c) shows the results of the TEM investigation on graphene-Au hybrid prepared by chemical synthesis as outlined in Section 2.4. The bright field micrograph (Figure 3(c)) shows uniform distribution of Au nanocrystals (appeared as dark dots) in the crumbled nanosheets of graphene. It is clearly visible that highly dispersed Au nanoparticles may provide large available surface area and enhance activities towards different reactions. The distribution of Au nanoparticles embedded in the graphene is shown as bottom inset of Figure 3(c). The average size of the particle is 8 ± 4 nm. The histogram indicates broad size distribution. The SADP pattern obtained from the hybrid is shown as upper inset of Figure 3(c). It

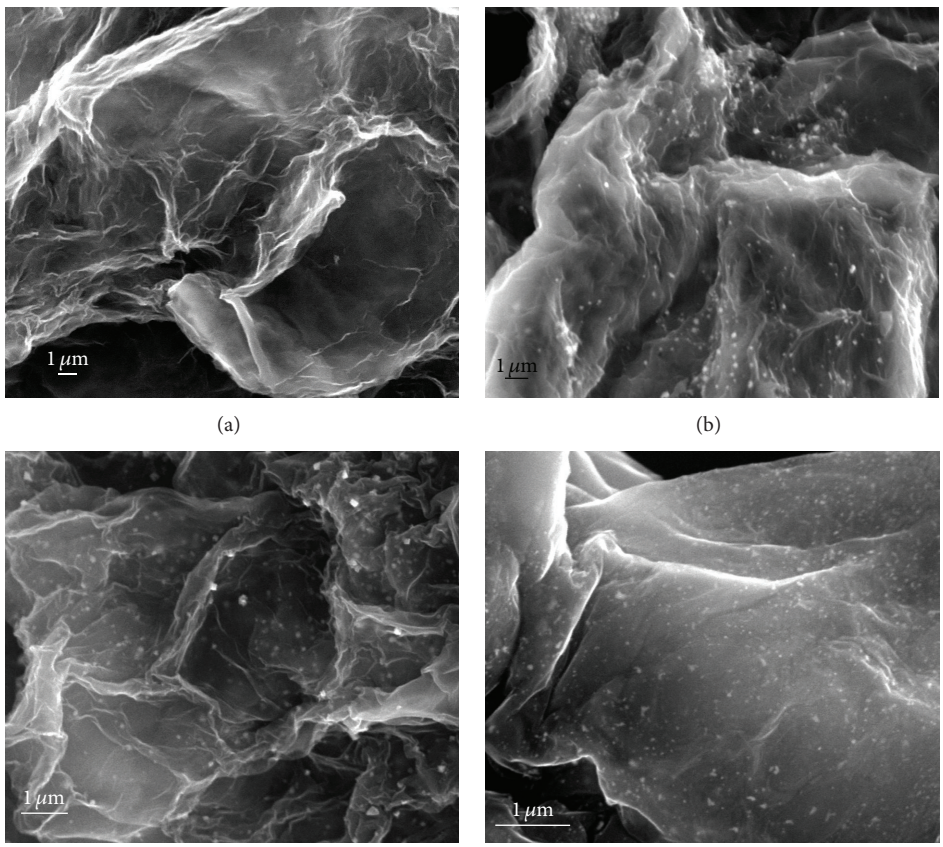

Figure 2: SEM image of (a) G, (b) Ag-G, (c) Au-G, and (d) Cu-G.

clearly reveals the diffraction rings corresponding to Au along with diffraction rings due to graphene. Figure 3(d) shows the bright field micrograph of graphene-Cu nanoparticle hybrid, revealing uniform distribution of Cu nanoparticle within the graphene sheets. The SADP pattern, as shown in the inset of the figure, confirms the presence of Cu. The detailed particle size analysis indicates that the average particle size is 6 ± 3 nm.

4.2. Optical Property Characterization. In the following, we shall describe and discuss the results obtained during optical property characterization of the graphene as well as graphene-metal nanoparticle hybrids. The optical properties of the graphene and hybrids are obtained using Raman and UV-Vis spectroscopy. From the earlier section, it is clear that the hybrids contain uniform distribution of Ag, Au, and Cu nanoparticles embedded in the graphene matrix. Therefore, it is worth to look into the optical properties of these hybrids. The discussion will be done by comparing the optical properties of monolithic graphene sheets with the hybrids.

4.2.1. Raman Spectroscopy. Figure 4(a) shows the Raman spectra of GO and graphene. The spectra reveal the presence of characteristics D (defect) and G (graphite) bands, 2D band, and (D + G) band. It is to be noted that D band arises due to in-plane stretching of sp^2-bonded carbon atoms in the hexagonal lattice, whereas G band is due to small graphitic domains because of vibrations of sp^3-bonded carbon atoms [28]. The 2D band originates due to second order two phonon process. Table 1 shows the detailed value of different bands in GO and graphene. For GO, D band is located at 1346 cm^{-1}, whereas G and 2D bands are located at 1590 cm^{-1} and 2697 cm^{-1}, respectively. The reduction of GO to graphene shows significant red shift in position of G (1579 cm^{-1}), D band (1340 cm^{-1}), and 2D band (2677 cm^{-1}) (Figure 4(a)). The red shift of G band in graphene is mainly due to the restoration of conjugated double bonds and the increase in the number of sp^2-bonded carbon atoms in the graphene during the reduction of GO. Table 1 also reports the ratio of the intensities of D and G bands (I_D/I_G) in GO (1.01) and graphene (1.09). It is to be noted that the ratio (I_D/I_G) is a measure of disordered carbon and normally expresses (sp^2/sp^3) carbon ratio [29]. It can be observed that I_D/I_G value increases from GO to graphene. The increase in the value indicates the relative increase of sp^2 domains and decrease of average crystallite size [30]. The ratio is found to be inversely proportional to the crystallite size (La):

$$\mathrm{La} = \left(2.4 \times 10^{-10}\right) \lambda_{\mathrm{laser}}^4 \left(\frac{I_D}{I_G}\right)^{-1}. \quad (1)$$

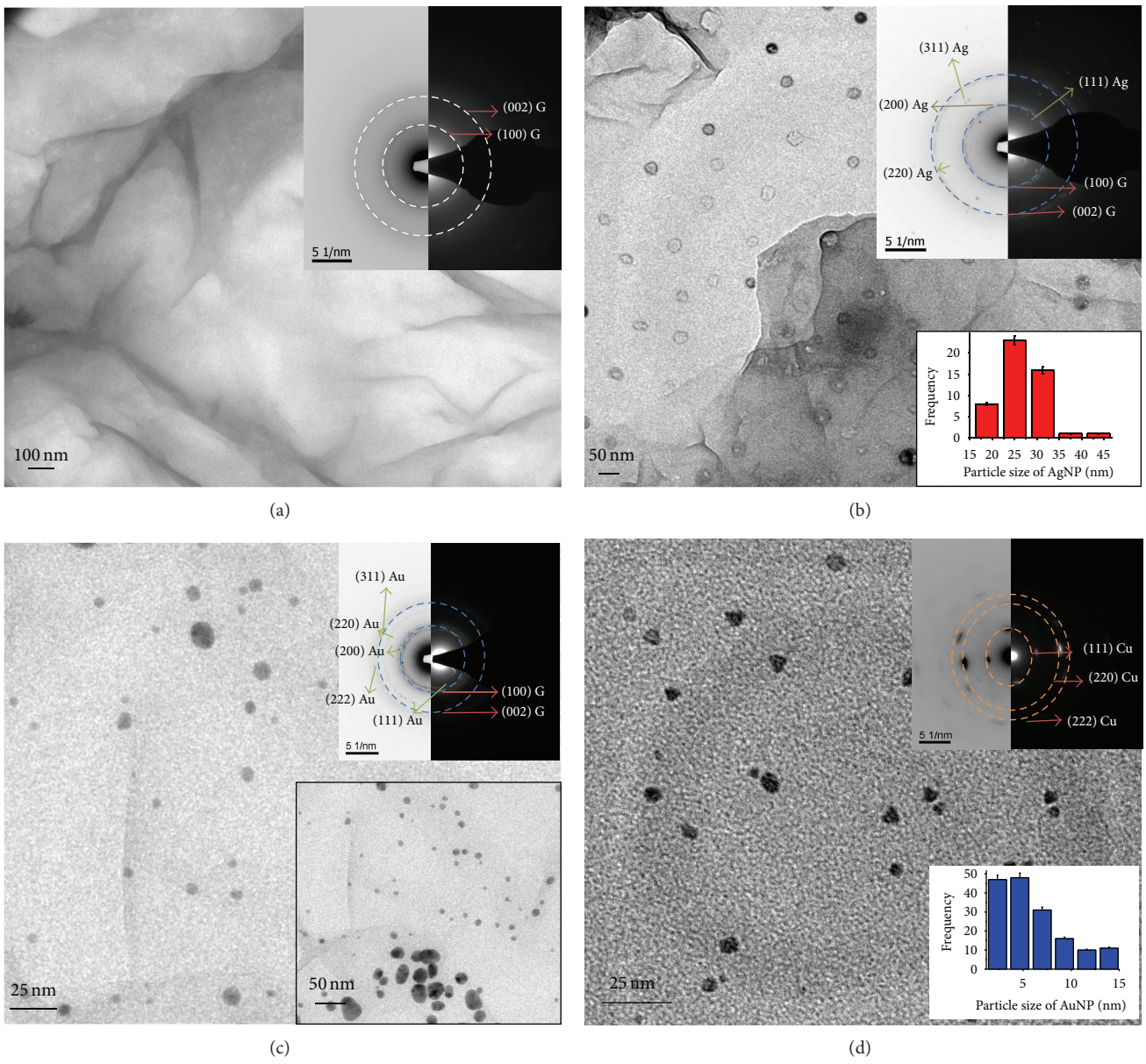

FIGURE 3: TEM micrographs and corresponding SAED patterns of (a) G, (b) Ag-G, (c) Au-G, and (d) Cu-G. The upper inset in each figure shows SAD pattern, whereas lower inset in figure (b) and (d) shows nanoparticle size distribution and in figure (c) shows low magnification bright field micrograph, revealing graphene sheets decorated with nanoparticles.

Using λ_{laser} = 514.5 nm, the calculated crystallite size of graphene is 18 nm.

Let us now discuss the case of graphene-metal nanoparticle hybrids. Figure 4(b) reveals Raman spectra of Ag-G, Au-G, and Cu-G hybrids. Table 1 shows detailed results of the positions of different vibrational bands as well as I_D/I_G values. The nature of the peaks of different bands, that is, D, G, 2D, and D + G bands, remains almost the same as that of monolithic graphene.

As indicated, G band is usually assigned to E_{2g} phonons of sp^2-bonded carbon atoms, whereas D band is assigned to breathing mode of k-phonon of A_{1g} symmetry. The position of G band does not change (Table 1) after the incorporation of metal nanoparticles. However, nature of shift is distinctly different in case of Cu-G as compared to Ag-G and Au-G. In case of Cu-G, the G band has undergone slight red shift (1578 cm^{-1}) as compared to graphene (1579 cm^{-1}). This indicates that the vibrational nature of small graphitic domain (sp^3-bonded carbon) has not been affected much by the presence of the metal nanoparticles. On the other hand, the position of D band in the hybrids has undergone blue shift as compared to graphene. The major shift has occurred in case of Cu-G (1351 cm^{-1}) indicating that the vibrational energy due to in-plane stretching of sp^2-bonded carbon is increased due to incorporation of metal nanoparticles. We believe that this is due to occupation of Cu atoms in specific position in

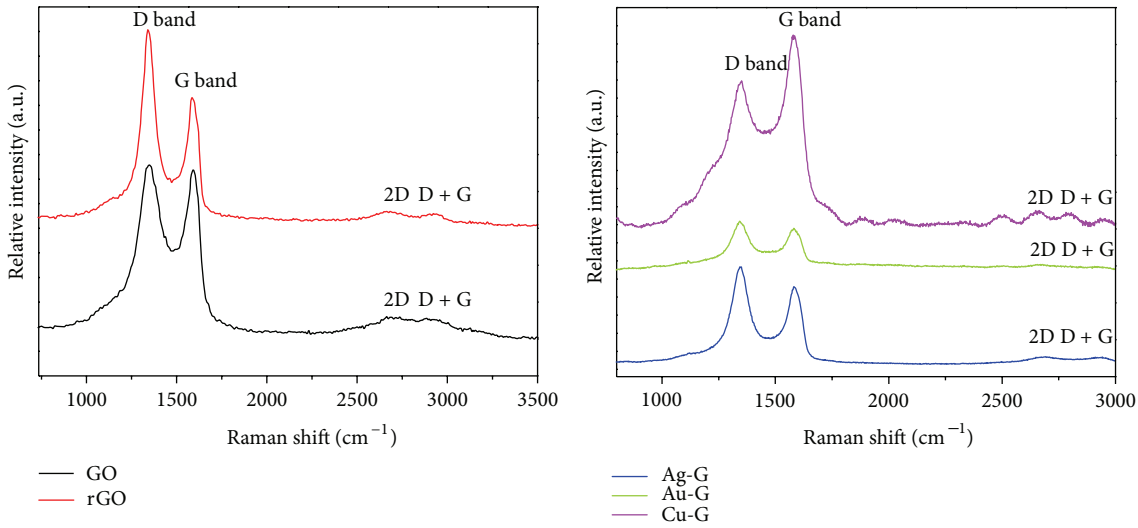

Figure 4: Raman spectra of (a) GO and G (b) Ag-G, Au-G, and Cu-G.

Table 1: Comparison of D, G, 2D, and (D + G) band positions and I_D/I_G value of GO, G, Ag-G Au-G, and Cu-G.

Material	D band	G band	2D band	D + G band	I_D/I_G value
Graphene oxide (GO)	1346 cm^{-1}	1590 cm^{-1}	2687 cm^{-1}	2919 cm^{-1}	1.01
Graphene (G)	1340 cm^{-1}	1579 cm^{-1}	2677 cm^{-1}	2912 cm^{-1}	1.09
Silver decorated graphene (Ag-G)	1346 cm^{-1}	1581 cm^{-1}	2690 cm^{-1}	2934 cm^{-1}	1.12
Gold decorated graphene (Au-G)	1342 cm^{-1}	1581 cm^{-1}	2667 cm^{-1}	2924 cm^{-1}	1.05
Copper decorated graphene (Cu-G)	1351 cm^{-1}	1578 cm^{-1}	2660 cm^{-1}	2949 cm^{-1}	0.89

the graphene structure, that is, in the hexagonal cage. These shifts in the position of G band may also be related to the position of nanoparticles that occupy the sites on the surface of graphene. As Cu has smaller atomic radius as compared to Ag and Au, we believe that Cu atoms may occupy the hexagonal cage of graphene, while Ag and Au occupy other adsorption sites T, (top on carbon atom) or B (bridge between two carbons). On the other hand, the shift in the position of D band is significantly larger in case of Cu-G as compared to that of Ag-G and Au-G. This may be due to larger distortion generated by occupation of Cu atoms in hexagonal cage of graphene than that generated by occupation of Ag and Au atoms on T or B site. Another important parameter characterizing the Raman spectra of hybrid is I_D/I_G ratio. This ratio has been found to increase from 1.09 to 1.12 in case of Ag-G, whereas it decreases in case of Au-G (1.05) and 0.89. The enhancement in the ratio indicates decrease in the site of in-plane sp^2 domain and partially ordered crystal structure of graphene nanosheets (GNs). On the other hand, the significant decrease in I_D/I_G ratio for Cu-G indicates that the new graphitic domains are more in number but smaller in size, formed upon reduction of GO to Cu-G.

Another important parameter of Raman spectroscopy is full width at half maxima (FWHM) of the D and G bands. Table 2 shows the results of GO, G, and graphene-metal nanoparticle hybrids. It is clearly observed that FWHM decreases substantially for Cu-G, whereas it does not change much for Au-G and Ag-G. On the other hand, FWHM of G band increases substantially for hybrids as compared to graphene. The most notable increase occurs in case of Cu-G. As the size of Cu NPs is smaller than Ag NPs and Au NPs, the local structural defect on the crystallite domains of graphene formed due to incorporation of Cu nanoparticles is lesser than those due to Ag and Au nanoparticles. The crystallite domain size of graphene calculated by using (1) for the Ag-G, Au-G, and Cu-G has been found to be 18 nm, 19 nm, and 22 nm, respectively. Therefore, as the crystallite size increases from Ag to Au to Cu, the FWHM value for D band shows decreasing trend.

Table 2: Comparison of FWHM of D and G band of GO, G, Ag-G, Au-G, and Cu-G.

Material	FWHM (D band)	FWHM (G band)
Graphene oxide (GO)	106 cm^{-1}	64 cm^{-1}
Graphene (G)	80 cm^{-1}	38 cm^{-1}
Silver decorated graphene (Ag-G)	81 cm^{-1}	67 cm^{-1}
Gold decorated graphene (Au-G)	78 cm^{-1}	63 cm^{-1}
Copper decorated graphene (Cu-G)	74 cm^{-1}	73 cm^{-1}

4.2.2. UV-Vis Spectroscopy. Another important optical characterization tool for graphene and graphene-related hybrids

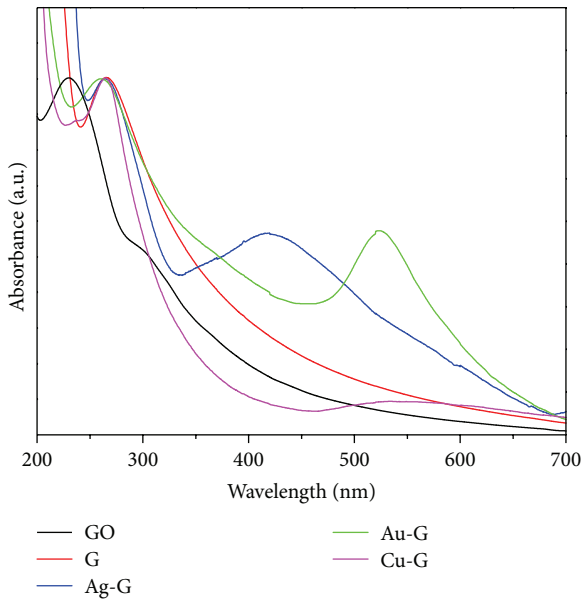

Figure 5: UV-Vis spectra of GO, G, Au-G, Ag-G, and Cu-G.

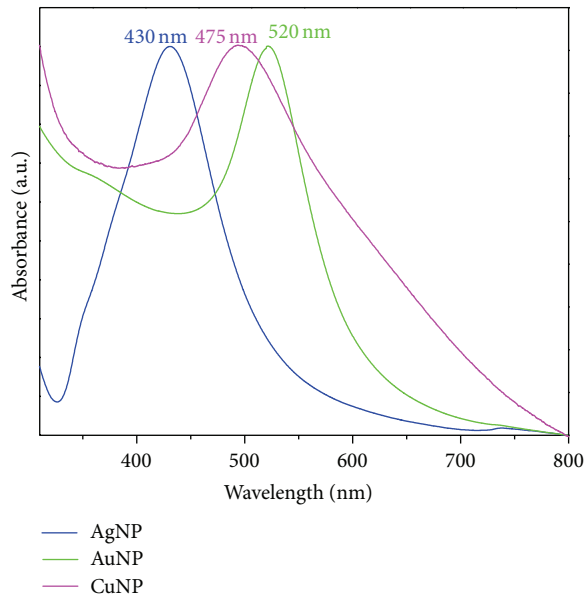

Figure 6: UV-Vis spectra of AgNP, AuNP, and CuNP.

is UV-Vis spectroscopy. Figures 5 and 6 summarize the UV-Vis spectroscopic observations in the present investigation. Detailed results are summarized in Table 3. Figure 5 reveals UV-Vis absorption spectra of graphene oxide (GO), graphene (G), graphene-metal nanoparticle hybrids, Ag-G, Au-G, and Cu-G. For GO, two characteristic peaks are observed in UV-Vis spectrum, a maximum at 230 nm, due to $\pi \rightarrow \pi^*$ transition of aromatic C-C bond and a shoulder at 303 nm, from $n \rightarrow \pi^*$ transition of C=O bond [31]. The original electronic conjugation is restored during reduction of GO to G by hydrazine hydrate, and a characteristic absorption peak of G has been observed at 266 nm, whereas the shoulder at 303 nm disappears. The incorporation of Ag NPs, in the G framework (Ag-G) is confirmed by the presence of absorption peak at 420 nm, which is considered to be due to surface plasmon resonance of Ag NPs. The bare Ag NPs derived from the reduction of Ag^+ by hydrazine hydrate under same condition is characterized by an absorption peak at 430 nm, which is consistent with previous studies [32, 33]. Clearly the incorporation of Ag NPs onto the stable aqueous graphene dispersion leads to blue shift of the surface plasmon resonance characteristics. It also has been observed that the absorption peak position of graphene for Ag-G hybrids changes to 260 nm, a blue shift of 6 nm as compared to aqueous graphene dispersion. The blue shift can be the result of charge transfer interaction between graphene and Ag NPs and has been confirmed by enhancement of Raman signals (Figure 4(b)). Similar measurements have been carried out for Au-G and Cu-G hybrids. The absorption peak of graphene in the Au-G is also blue shifted, by 4 nm. Therefore, charge transfer interaction between graphene and Au is poor as compared to Ag-G. The similar observation has been made for absorption peak of graphene in case of Cu-G. Table 3 also reveals that the surface plasmon resonance of Cu NPs is affected strongly by graphene nanosheets as plasmon resonance has red shifted by 65 nm. On the other hand, the surface plasmon resonance of Au NPs has undergone red shift only by 4 nm as compared to free Au NPs. Therefore, the behavior of metal NPs can be modified extensively by incorporating them into the graphene nanosheets. Obviously these interactions depend on the position of these NPs, where they occupy the hexagonal graphene framework. This will be investigated further.

Table 3: Comparison of UV-Vis absorption peak position of GO, G, AgNPs, Ag-G, AuNPs, Au-G, CuNPs, and Cu-G.

Material	Graphene peak position	Plasmon peak position
Graphene oxide (GO)	230 nm ($\pi \rightarrow \pi^*$) 303 nm ($n \rightarrow \pi^*$)	—
Graphene (G)	266 nm	—
Pure silver nanoparticles (AgNP)	—	430 nm
Silver decorated graphene (Ag-G)	260 nm	420 nm
Pure gold nanoparticles (AuNP)	—	520 nm
Gold decorated graphene (Au-G)	264 nm	524 nm
Pure copper nanoparticles (CuNP)	—	475 nm
Copper decorated graphene (Cu-G)	264 nm	540 nm

5. Summary

The present investigation has categorically shown that it is possible to synthesize graphene-metal nanoparticle hybrids in aqueous media by chemical rule. The following conclusion can be drawn from the study.

(a) Fine nanoparticles (Ag, Au, and Cu) decorated graphene can be prepared by chemical synthesis. The size of the nanoparticles varies from 5 to 35 nm.

(b) The G and D bands can be modified more extensively by Cu than Ag or Au.

(c) The surface plasmon resonance of the metal nanoparticles can be altered by incorporation of nanoparticles in the graphene nanosheets.

(d) The electronic interaction between the metal nanoparticle and graphene depends on the type of metal as well as size of the atom.

Acknowledgments

This work was supported by research funding from Department of Science and Technology (DST), the Government of India. The authors would like to acknowledge the usage of Electron Microscopy facility (SEM, TEM), XRD facility Raman Spectroscopy facility, FTIR facility, and UV-Vis spectroscopy facility at IIT Kanpur. The authors would like to thank Indian National Science Academy for funding for making the paper as open access.

References

[1] A. K. Geim and K. S. Novoselov, "The rise of graphene," *Nature Materials*, vol. 6, no. 3, pp. 183–191, 2007.

[2] X. Huang, Z. Yin, S. Wu et al., "Graphene-based materials: synthesis, characterization, properties, and applications," *Small*, vol. 7, no. 14, pp. 1876–1902, 2011.

[3] C. Lee, X. Wei, J. W. Kysar, and J. Hone, "Measurement of the elastic properties and intrinsic strength of monolayer graphene," *Science*, vol. 321, no. 5887, pp. 385–388, 2008.

[4] A. A. Balandin, S. Ghosh, W. Bao et al., "Superior thermal conductivity of single-layer graphene," *Nano Letters*, vol. 8, no. 3, pp. 902–907, 2008.

[5] K. I. Bolotin, K. J. Sikes, Z. Jiang et al., "Ultrahigh electron mobility in suspended graphene," *Solid State Communications*, vol. 146, no. 9-10, pp. 351–355, 2008.

[6] M. D. Stoller, S. Park, Z. Yanwu, J. An, and R. S. Ruoff, "Graphene-based ultracapacitors," *Nano Letters*, vol. 8, no. 10, pp. 3498–3502, 2008.

[7] D. A. Areshkin and C. T. White, "Building blocks for integrated graphene circuits," *Nano Letters*, vol. 7, no. 11, pp. 3253–3259, 2007.

[8] U. Khan, P. May, A. O'Neill, and J. N. Coleman, "Development of stiff, strong, yet tough composites by the addition of solvent exfoliated graphene to polyurethane," *Carbon*, vol. 48, no. 14, pp. 4035–4041, 2010.

[9] J. Y. Liu and R. H. Hurt, "Ion release kinetics and particle persistence in aqueous nano-silver colloids," *Environmental Science and Technology*, vol. 44, no. 6, pp. 2169–2175, 2010.

[10] M. Pumera, "Graphene-based nanomaterials and their electrochemistry," *Chemical Society Reviews*, vol. 39, no. 11, pp. 4146–4157, 2010.

[11] X. Lu, M. Yu, H. Huang, and R. S. Ruoff, "Tailoring graphite with the goal of achieving single sheets," *Nanotechnology*, vol. 10, no. 3, pp. 269–272, 1999.

[12] M. Eizenberg and J. M. Blakely, "Carbon monolayer phase condensation on Ni(111)," *Surface Science*, vol. 82, no. 1, pp. 228–236, 1979.

[13] S. Stankovich, D. A. Dikin, R. D. Piner et al., "Synthesis of graphene-based nanosheets via chemical reduction of exfoliated graphite oxide," *Carbon*, vol. 45, no. 7, pp. 1558–1565, 2007.

[14] S. Niyogi, E. Bekyarova, M. E. Itkis, J. L. McWilliams, M. A. Hamon, and R. C. Haddon, "Solution properties of graphite and graphene," *Journal of the American Chemical Society*, vol. 128, no. 24, pp. 7720–7721, 2006.

[15] L.-X. Li, B.-G. An, H. Nishihara et al., "Water-dispersible "carbon nanopods" with controllable graphene layer orientation," *Chemical Communications*, no. 30, pp. 4554–4556, 2009.

[16] Y.-K. Kim, H.-K. Na, and D.-H. Min, "Influence of surface functionalization on the growth of gold nanostructures on graphene thin films," *Langmuir*, vol. 26, no. 16, pp. 13065–13070, 2010.

[17] K. Jasuja and V. Berry, "Implantation and growth of dendritic gold nanostructures on graphene derivatives: electrical property tailoring and Raman enhancement," *ACS Nano*, vol. 3, no. 8, pp. 2358–2366, 2009.

[18] J. Li and C.-Y. Liu, "Ag/Graphene heterostructures: synthesis, characterization and optical properties," *European Journal of Inorganic Chemistry*, no. 8, pp. 1244–1248, 2010.

[19] N. Tian, Z.-Y. Zhou, S.-G. Sun, Y. Ding, and L. W. Zhong, "Synthesis of tetrahexahedral platinum nanocrystals with high-index facets and high electro-oxidation activity," *Science*, vol. 316, no. 5825, pp. 732–735, 2007.

[20] B. Lim, M. Jiang, P. H. C. Camargo et al., "Pd-Pt bimetallic nanodendrites with high activity for oxygen reduction," *Science*, vol. 324, no. 5932, pp. 1302–1305, 2009.

[21] S. Chu, L. Hu, X. Hu, M. Yang, and J. Deng, "Titanium-embedded graphene as high-capacity hydrogen-storage media," *International Journal of Hydrogen Energy*, vol. 36, no. 19, pp. 12324–12328, 2011.

[22] D. Astruc, F. Lu, and J. R. Aranzaes, "Nanoparticles as recyclable catalysts: the frontier between homogeneous and heterogeneous catalysis," *Angewandte Chemie—International Edition*, vol. 44, no. 48, pp. 7852–7872, 2005.

[23] A. Y. Stakheev and L. M. Kustov, "Effects of the support on the morphology and electronic properties of supported metal clusters: modern concepts and progress in 1990s," *Applied Catalysis A*, vol. 188, no. 1-2, pp. 3–35, 1999.

[24] W. Yuana, Y. Gua, and L. Li, "Green synthesis of graphene/Ag nanocomposites," *Applied Surface Science*, vol. 261, pp. 753–758, 2012.

[25] K. S. Subrahmanyam, A. K. Manna, S. K. Pati, and C. N. R. Rao, "A study of graphene decorated with metal nanoparticles," *Chemical Physics Letters*, vol. 497, no. 1–3, pp. 70–75, 2010.

[26] W. S. Hummers Jr. and R. E. Offeman, "Preparation of graphitic oxide," *Journal of the American Chemical Society*, vol. 80, no. 6, p. 1339, 1958.

[27] A. Mao, D. Zhang, X. Jin et al., "Synthesis of graphene oxide sheets decorated by silver nanoparticles in organic phase and their catalytic activity," *Journal of Physics and Chemistry of Solids*, vol. 73, pp. 982–986, 2012.

[28] H.-S. Zhang and K. Komvopoulos, "Direct-current cathodic vacuum arc system with magnetic-field mechanism for plasma stabilization," *Review of Scientific Instruments*, vol. 79, no. 7, Article ID 073905, 2008.

[29] A. C. Ferrari and J. Robertson, "Interpretation of Raman spectra of disordered and amorphous carbon," *Physical Review B*, vol. 61, no. 20, pp. 14095–14107, 2000.

[30] F. Tuinstra and J. L. Koenig, "Raman spectrum of graphite," *Journal of Chemical Physics*, vol. 53, no. 3, pp. 1126–1130, 1970.

[31] N. Tian, Z.-Y. Zhou, S.-G. Sun, Y. Ding, and L. W. Zhong, "Synthesis of tetrahexahedral platinum nanocrystals with high-index facets and high electro-oxidation activity," *Science*, vol. 316, no. 5825, pp. 732–735, 2007.

[32] I. A. Wani, S. Khatoon, A. Ganguly, J. Ahmed, A. K. Ganguli, and T. Ahmad, "Silver nanoparticles: Large scale solvothermal synthesis and optical properties," *Materials Research Bulletin*, vol. 45, no. 8, pp. 1033–1038, 2010.

[33] I. Pastoriza-Santos and L. M. Liz-Marzán, "Reduction of silver nanoparticles in DMF. Formation of monolayers and stable colloids," *Pure and Applied Chemistry*, vol. 72, no. 1-2, pp. 83–90, 2000.